HHS Public Access

Author manuscript

Cell Rep. Author manuscript; available in PMC 2024 February 01.

Published in final edited form as:

Cell Rep. 2023 December 26; 42(12): 113533. doi:10.1016/j.celrep.2023.113533.

Cerebellar contribution to autism-relevant behaviors in fragile X syndrome models

Jennifer M. Gibson[1,2], **Anthony Hernandez Vazquez**[1,2], **Kunihiko Yamashiro**[1], **Vikram Jakkamsetti**[1], **Chongyu Ren**[1], **Katherine Lei**[1], **Brianne Dentel**[1,3], **Juan M. Pascual**[1,3], **Peter T. Tsai**[1,2,3,4,5,*]

[1]Department of Neurology, University of Texas Southwestern Medical Center, Dallas, TX 75390, USA

[2]Department of Neuroscience, University of Texas Southwestern Medical Center, Dallas, TX 75390, USA

[3]Department of Pediatrics, University of Texas Southwestern Medical Center, Dallas, TX 75390, USA

[4]Department of Psychiatry, University of Texas Southwestern Medical Center, Dallas, TX 75390, USA

[5]Lead contact

SUMMARY

Cerebellar dysfunction has been linked to autism spectrum disorders (ASDs). Although cerebellar pathology has been observed in individuals with fragile X syndrome (FXS) and in mouse models of the disorder, a cerebellar functional contribution to ASD-relevant behaviors in FXS has yet to be fully characterized. In this study, we demonstrate a critical cerebellar role for *Fmr1* (*fragile X messenger ribonucleoprotein 1*) in ASD-relevant behaviors. First, we identify reduced social behaviors, sensory hypersensitivity, and cerebellar dysfunction, with loss of cerebellar *Fmr1*. We then demonstrate that cerebellar-specific expression of *Fmr1* is sufficient to impact social, sensory, cerebellar dysfunction, and cerebro-cortical hyperexcitability phenotypes observed in global *Fmr1* mutants. Moreover, we demonstrate that targeting the ASD-implicated cerebellar region Crus1 ameliorates behaviors in both cerebellar-specific and global *Fmr1* mutants. Together, these results demonstrate a critical role for the cerebellar contribution to FXS-related behaviors, with implications for future therapeutic strategies.

*Correspondence: peter.tsai@utsouthwestern.edu.

AUTHOR CONTRIBUTIONS

J.M.G. and P.T.T. designed the study. J.M.G., P.T.T., A.H.V., C.R., B.D., and K.Y. performed experiments. J.M.G., P.T.T., V.J., A.H.V., and C.R. analyzed data. J.M.G. wrote the first draft of the paper, and J.M.G., J.M.P., V.J., and P.T.T. edited and finalized the manuscript.

SUPPLEMENTAL INFORMATION

Supplemental information can be found online at https://doi.org/10.1016/j.celrep.2023.113533.

DECLARATION OF INTERESTS

The authors declare no competing interests.

In brief

Gibson et al. demonstrate that loss of cerebellar *Fmr1* leads to reduced social behaviors, sensory hypersensitivity, and cerebellar dysfunction. In global *Fmr1* mutants, cerebellar-specific expression of *Fmr1* is sufficient to alter observed phenotypes. Moreover, targeting the ASD-implicated cerebellar region Crus1 ameliorates behaviors in both cerebellar-specific and global *Fmr1* mutants.

Graphical Abstract

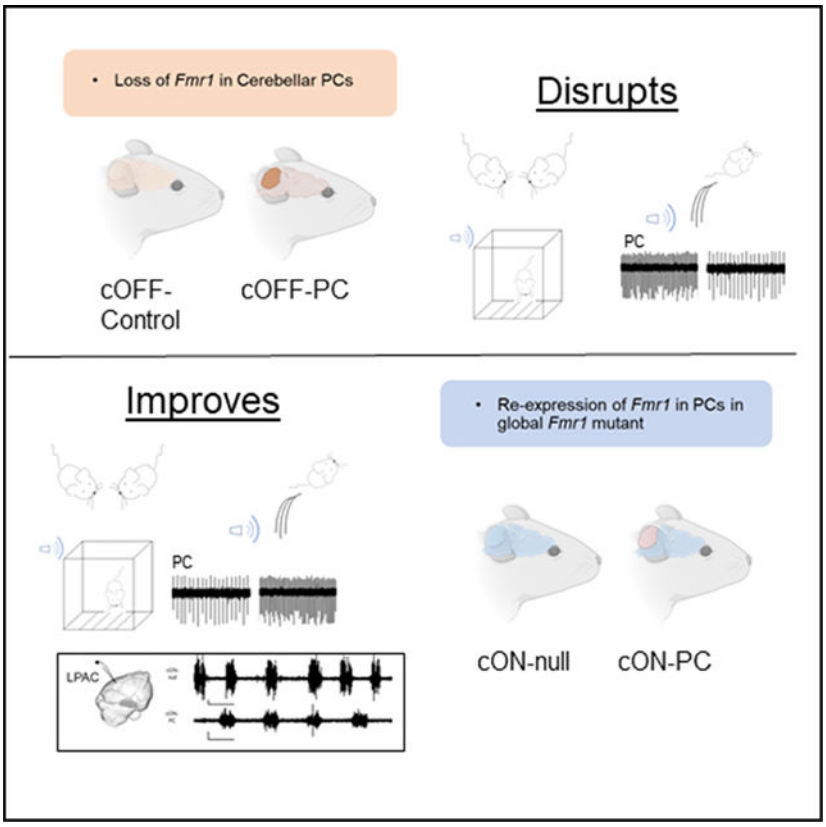

INTRODUCTION

Autism spectrum disorders (ASDs) are behaviorally diagnosed using characteristics such as challenges in social communication, restrictive/repetitive behaviors, and sensory hypersensitivity; however, underlying mechanisms contributing to ASDs remain unclear. ASDs have a clear but complex genetic contribution.[1–4] Among the most prevalent monogenic contributions to ASD is fragile X syndrome (FXS).[4] FXS results from trinucleotide repeat expansion in the *Fmr1* gene, resulting in hypermethylation and inhibition of the gene.[5] FXS accounts for up to 1%–2% of all cases of ASD[6] and is also associated with intellectual disability, anxiety, and sensory hypersensitivity.[7] Investigations into the pathogenesis of FXS have identified critical roles for *Fmr1* in protein translation, enhanced synaptic plasticity, and cortical hyper-excitability in FXS models.[8–10] Hyperexcitability is further supported by electroencephalogram (EEG) studies in individuals

with FXS where heightened cortical arousal is reliably observed in frontal and parietal association cortices.[11] Also, consistent UP states in the somatosensory cortex have been found in animal models,[12] in addition to heightened neocortical synchrony.[13]

However, a growing body of literature in ASD and FXS has implicated brain mechanisms beyond the cerebral cortex. Subcortical and specifically cerebellar regions have been increasingly associated with ASD-related behaviors. In fact, the most consistently identified pathology in postmortem studies of ASD is loss of Purkinje cells (PCs), the sole output neurons of the cerebellar cortex.[14–16] Additionally, investigations utilizing volumetric, diffusion, functional imaging, and investigations using multiple animal models consistently highlight cerebellar dysfunction in ASD.[17–19] Moreover, studies of cerebellar-specific mutants of other genetic disruptions linked to ASD have further implicated the cerebellum.[20–28]

Cerebellar abnormalities have been observed in individuals with FXS as well as in "pre-mutation" carriers manifesting fragile X-associated tremor/ataxia syndrome (FXTAS).[29,30] Specific examination of loss of *Fmr1* in PCs revealed enhanced synaptic plasticity in the cerebellum,[31] akin to the enhanced plasticity observed in cerebral cortical[13] and hippocampal[8] circuits in FXS models. Additionally, studies have revealed cerebellar interneuron regulation of PC firing frequencies in FXS models.[32] Together, these data point to cerebellar involvement in FXS; however, the contribution of the cerebellum to ASD-related behaviors in FXS has not been well studied.

RESULTS

PC *Fmr1* is necessary for social behaviors

Fmr1 expression is fairly ubiquitous, with expression throughout the body and high expression throughout the brain.[33] To evaluate the cerebellar contribution of *Fmr1* to ASD behaviors, we generated a mutant mouse with conditional deletion of *Fmr1* in cerebellar PCs ($L7^{Cre+}$;$Fmr1^{flox/flox}$ [referred to as cOFF-PCs]), generously provided by Dr. David Nelson (Baylor College of Medicine, Houston, TX, USA) (Figure S1A).[34] As *Fmr1* is on the X chromosome and FXS is more often observed in males compared to females, these studies were conducted solely in male mice. All studies were performed blinded to genotype. To investigate social behavior, we first performed social approach and social novelty testing using the three-chambered apparatus (Figure 1A). In the social approach paradigm, when presented with a novel social stimulus, cOFF-control mice show a significant preference for the novel animal over the novel object; however, deletion of *Fmr1* in the PCs of cOFF-PC mice resulted in a lack of social preference (Figures 1B and 1C). In social novelty testing, cOFF-control mice also prefer the novel animal over the familiar animal, while cOFF-PC mutants show no such preference (Figures 1B and 1C). We further tested social behaviors using a social olfactory paradigm. As social behaviors are critically dependent on olfactory abilities, we evaluated responses to both non-social and social olfactory stimuli. We did not observe any olfactory deficits between the cOFF-PC mutants and cOFF-controls during investigations of the non-social scents (Figure 1D). However, when presented with the social olfactory stimulus, cOFF-PC mice spent less time investigating the social scent when compared to cOFF-controls (Figure 1D), consistent with a specific social deficit. In each

sociability test, cOFF-PC mutant mice displayed no preference for social stimuli, suggesting that *Fmr1* in PCs is necessary for the manifestation of social behaviors.

Restrictive and repetitive behaviors commonly identified in ASD are also a feature exhibited by individuals with FXS.[35] To test for these behavioral correlates in mice, we examined repetitive behaviors using a grooming assay. We did not observe differences in time spent grooming in the cOFF-PC mice compared to littermate controls (Figure 1E). However, upon examination of behavioral flexibility using the water Y maze, we found that cOFF-PC mice had significant difficulty re-learning the location of the platform in the water Y maze despite their ability to learn the initial platform location comparable to control littermates (Figure 1F). These specific deficits in the reversal learning component of the assay are indicative of behavioral inflexibility.

Another diagnostic criterion for ASD is sensory hypersensitivity, a finding frequently identified in individuals with FXS.[36–39] Animal models of FXS have audiogenic seizures (AGSs) and demonstrate hypersensitivity to acoustic stimuli.[40–42] We tested for AGS in cOFF-PC mutants and control littermates yet did not observe any significant changes ($p = 0.0678$) between genotypes (Figure 1G). We further evaluated sensory responsiveness through their acoustic startle response, another test of auditory sensitivity. cOFF-PC mice and their littermate cOFF-controls were exposed to varying intensities of acoustic stimuli at random intervals. We found that the cOFF-PC mutants have a significantly enhanced startle response at higher decibels (Figure 1H).

Individuals with FXS also exhibit abnormal brain activation in response to fear memories,[43] and FXS animal models show deficits in associative memory tasks.[44] Although less well understood, the cerebellum has been linked to enabling and storing fear memories[45] and has clear roles in associative learning paradigms.[46,47] Consequently, to evaluate a cerebellar *Fmr1* contribution, we tested the ability of cOFF-PC mutants to acquire, store, and recall a fear memory over a 3-day fear conditioning test. No differences were observed in any of the 3 testing phases (Figures 1I–1K), demonstrating that cerebellar *Fmr1* is not necessary for fear-conditioned learning.

To verify that any observed behaviors were not due to altered motor or anxiety-like behaviors, we evaluated performance on rotarod, open field, and elevated plus maze. We did not observe any significant changes in locomotor capabilities or response to anxiogenic environments between groups (Figures S1B–S1F).

Taken together, these results show that loss of *Fmr1* in cerebellar PCs leads to reduced social preference, behavioral inflexibility, and hypersensitivity to auditory stimuli, revealing *Fmr1* in PCs as necessary for normal manifestation of these ASD-relevant behaviors in FXS.

Loss of *Fmr1* in PCs leads to cerebellar dysfunction

PC loss is a consistent phenotype in ASD[48,49] and has been identified in other cerebellar models of autism-linked genes.[20,50,51] We therefore evaluated whether PC loss might be observed in cOFF-PC mutants and thus contribute to phenotypes observed in these mutants.

However, we did not observe any significant alterations in PC number in cOFF-PC mice compared to cOFF-controls (Figures 1L and 1M).

In addition to cell number, cerebellar function is altered in mouse models of ASD-linked genes,[21,50] consistent with studies in individuals with ASD showing cerebellar dysfunction.[52,53] Similarly, prior studies in cOFF-PC mice have demonstrated alterations in synaptic plasticity.[31] However, examination of PC intrinsic properties has not been studied extensively in cOFF-PC mice. We sought to test the intrinsic physiological properties of PCs lacking expression of *Fmr1* as a measure of PC function. We tested spontaneous activity using extracellular recordings in addition to intrinsic excitability in acute slice preparations and found decreased spontaneous activity and excitability, indicative of reduced cerebellar function in this model (Figures 1N and 1O).

Chemogenetic activation of PC activity in RCrus1 is sufficient to improve social preferences in cOFF-PC mutants

Human imaging studies have implicated cerebellar right crus1 (RCrus1) in social behavior,[54] and structural alterations of this region are identified in individuals with ASD.[19] We have previously demonstrated that chemogenetic modulation of PC excitability in RCrus1 can improve sociability in a conditional cerebellar *Tsc1* mutant.[24] As we observed reduced PC excitability in cOFF-PC mutants (Figures 1N and 1O), we hypothesized that chemogenetic activation of RCrus1 PCs might similarly improve ASD-related behavioral challenges observed in *Fmr1* cOFF-PC mutants.

We injected adeno-associated virus (AAV)8-calcium/calmodulin-dependent protein kinase (CaMK)IIα-hM3D(Gq)-mCherry or AAV8-CaMKIIα-enhanced green fluorescent protein (EGFP) (virus control), which selectively target cerebellar PCs, into RCrus1 of cOFF-PC mutants. Injection site accuracy and infection specificity to PCs were histologically verified (Figures S2A and S2B). We also confirmed activation of PCs after successful uptake of the virus by recording from acute cerebellar slices, and we observed increased firing frequency in response to clozapine-N-oxide (CNO) in infected PCs (Figure S2C).

After infection with virus containing Gq or GFP and sufficient time for animals to recover from surgical procedures, we administered vehicle (VEH) or CNO intraperitoneally to Gq- or GFP-injected cOFF-PC mice. With chemogenetic stimulation of excitability, we observed an increase in social preference during social approach, social novelty, and social olfactory testing that was absent in all GFP-injected and VEH-treated groups (Figures 2A–2C). However, when we tested restrictive and repetitive behaviors, CNO-driven activation of RCrus1 PCs was not sufficient to alter grooming time or improve reversal learning in the water Y maze (Figures 2D and 2E).

Imaging studies have identified lateral cerebellar involvement in startle behaviors.[54] To investigate whether modulation of RCrus1 is sufficient to improve the heightened acoustic sensitivity previously observed during acoustic startle testing in the cOFF-PC mice, we tested the acoustic startle response in mice with Gq or GFP injected into *Fmr1* cOFF-PC mice. With activation of RCrus1 PCs, cOFF-PC mice showed reduced startle response to auditory stimuli as compared to other cohorts (Figure 2F). These data suggest that

modulation of RCrus1 PCs alone is sufficient to reduce the enhanced startle phenotype observed in cOFF-PC mutants.

We then tested whether modulation of RCrus1 might also be sufficient to improve associative learning in this model. We evaluated performance in the 3-day fear conditioning tasks; following CNO administration, there was no observable difference with stimulation of RCrus1 PCs compared with other treatment cohorts (Figures 2G–2I). Furthermore, CNO administration with RCrus1-Gq infection did not affect performance on the rotarod, elevated plus maze, or open field, continuing to lend support for a lack of motor abnormalities or anxiety-like behaviors (Figures S3A–S3E).

Taken together, these data show that targeting PC activity in cerebellar domain RCrus1 is sufficient to improve the impaired sociability and sensory behaviors observed in cOFF-PC mutants without significantly affecting restrictive, repetitive, or associative learning behaviors.

Expression of *Fmr1* in PCs prevents the development of social deficits in global *Fmr1* mutants

We then wanted to ask whether *Fmr1* expression in PCs might also be sufficient to maintain behaviors in an otherwise global *Fmr1* mutant. In addition to potential mechanistic insights, these experiments also might offer insights in a more translationally relevant manner, as individuals with FXS and individuals with ASD in general are unlikely to present with cerebellar-specific genetic abnormalities. Thus, we sought a more translationally relevant global mutant model to ask whether restoring cerebellar *Fmr1* specifically would be sufficient to modify phenotypes in a global FXS mutant background. To evaluate this question, we examined whether re-expression of *Fmr1* solely in cerebellar PCs would improve behavioral deficits in a model of *Fmr1* global loss. To achieve this, we used a *Fmr1* conditional ON model (cON-null)[10] generously provided by Dr. David Nelson (Baylor College of Medicine), where *Fmr1* is only expressed in the presence of Cre recombinase. We crossed *L7/Purkinje cell protein* (*Pcp*)*2-Cre* mice with the cON mice to generate a model where *Fmr1* is expressed only in PCs (referred to as cON-PCs). These mice were compared with *L7/Pcp2-Cre*-negative littermates (cON-null), which do not express *Fmr1* (Figure S4A), in addition to control littermates that are *L7/Pcp2-Cre* positive but are wild type for the *Fmr1* gene (cON-wild type).

Studies of other constitutive *Fmr1* mutants have identified deficits in social and repetitive behaviors.[55,56] However, no studies on constitutive cON-null mutants have examined ASD-relevant behaviors. We observed social deficits in cON-null mice using the three-chamber social approach and social novelty tests when compared with cON-wild-type controls (Figures 3A and 3B). We then examined whether expression of *Fmr1* in PCs might alter these behaviors. In fact, with expression of PC *Fmr1* in the cON-PC cohort, social preference was observed in both paradigms (Figures 3A and 3B). Similarly, with social olfactory testing, cON-PC mice investigated the scents for a significantly longer amount of time, whereas cON-null mice spent comparably less time investigating a novel social scent (Figure 3C).

We then tested for repetitive behaviors or behavioral inflexibility in cON mutant mice. However, in grooming and water Y-maze tests, we did not observe repetitive behaviors or behavioral inflexibility in the cON-null mice. Further, these behaviors remained unaffected in the cON-PC mice where *Fmr1* is expressed in PCs, and behavior remained markedly similar to the cON-wild type (Figures 3D and 3E).

Auditory hypersensitivity, AGS in particular, is one of the most robust phenotypes observed in constitutive FXS mouse models,[40,57] and thus we sought to examine sensory hypersensitivity with this paradigm. We observed increased AGS in our cON-null global mutants as evidenced by high scores in AGS testing in comparison with cON-wild-type mice. As with social behavior, this phenotype was significantly improved in the cON-PC mice (Figure 3F). Consistent with this change in sensory hypersensitivity, in acoustic startle testing, we similarly show an increased acoustic startle response in cON-null mutants compared to cON-wild-type controls. As with AGS, expression of *Fmr1* in PCs in cON-PC mice results in startle responses comparable to cON-wild types (Figure 3G). Together, these data indicate that expression of *Fmr1* in PCs is sufficient to improve sensory hypersensitivity observed upon constitutive loss of *Fmr1*.

We then tested these mice for abnormalities in fear memory. Global *Fmr1* knockout (KO) mice exhibit altered contextual memory often considered to result from hippocampal and amygdala circuits affected by loss of *Fmr1*.[58] All groups demonstrated increases in freezing behavior during the acquisition of the fear memory (tone/shock), though the cON-wild-type and cON-PC responses were heightened (Figure 3H). Examination of their ability to recall the association in the same context did not differ significantly between groups (Figure 3I). Yet, in cued testing, we observed significantly reduced freezing times in cON-null cohorts as compared to cON-wild-type cohorts. Re-expression of *Fmr1* in PCs in cON-PC mice resulted in increased freezing times following the cued tone (Figure 3J). These data indicate that expression of *Fmr1* in PCs improves impairments in associative learning observed with constitutive loss of *Fmr1*.

In all groups, we also did not observe any differences between groups in rotarod, elevated plus maze, or open field assays, supporting a conclusion that changes in observed behaviors were not secondary to changes in locomotor and/or anxiety-like behaviors (Figures S4B–S4F). Taken together, these data further demonstrate an important role for cerebellar *Fmr1* in ASD-relevant behaviors and that expression of *Fmr1* in PCs in the setting of an otherwise global loss of *Fmr1* is sufficient for improvement in social behaviors, a decrease in sensory hypersensitivity, and an increase in associative fear learning.

Fmr1 expression in PCs restores PC function in *Fmr1* global mutants

We next evaluated mechanisms that might contribute to these behavioral impacts. As noted earlier, PC loss is a consistent phenotype in individuals with ASD and has been identified in postmortem analyses of individuals with FXS.[16] We thus quantified PC number following constitutive loss of *Fmr1*. However, no significant PC loss was observed in any of the groups (Figures 3K and 3L).

As excitability mechanisms have been implicated in cerebellar regulation of ASD-relevant behaviors,[24,31] we examined whether PC firing rates and excitability might contribute to observed phenotypes following global loss of *Fmr1*. In acute slice preparations, consistent with previous studies,[32] PC firing rates are reduced in cON-null mice compared to cON-wild-type control cohorts. We then examined whether expression of *Fmr1* in PCs might result in amelioration of these PC excitability deficits. We found that PCs in cON-PC mutants demonstrated firing rates and excitability that were significantly greater than cON-nulls and comparable to cON-wild-type control cohorts (Figures 3M and 3N).

Chemogenetic activation of RCrus1 PCs in a global *Fmr1* mutant ameliorates behavioral changes

We were able to ameliorate ASD phenotypes in a model of constitutive *Fmr1* loss through specific expression of *Fmr1* in cerebellar PCs. Therefore, we next asked if specifically targeting PCs solely in RCrus1 might be sufficient to improve behaviors, not just in cerebellar-specific models but also in a more translationally relevant constitutive, global *Fmr1* model. To test this question, we delivered DREADDs (either AAV8-CaMKIIα-hM3D(Gq)-mCherry or AAV8-CaMKIIα-EGFP control) to RCrus1 in cON-null mice to chemogenetically target PCs in RCrus1. After sufficient time for recovery, behaviors were evaluated starting at 6 weeks of age. As in previous chemogenetic experiments, CNO or VEH was administered 30 min prior to behavior testing. We evaluated social preference in the three-chamber social approach and social novelty assays. With CNO administration, we observed significantly increased time spent investigating the novel social stimulus in the RCrus1-Gq-infected group, which was not present in the VEH-treated or GFP-infected groups in social approach or novelty testing (Figures 4A and 4B). We see a similar finding in olfactory testing, with improvement in response to social olfactory cues and stable responses to non-social olfactory cues (Figure 4C). In contrast, we did not observe any differences in grooming behavior or performance on the water Y maze following CNO or VEH treatment (Figures 4D and 4E).

We then examined whether auditory sensory hypersensitivity could also be modulated by RCrus1 stimulation. We observed that activation of RCrus1 PCs in the cON-null model lowered the startle responses to acoustic stimuli as compared to VEH-treated Gq-infected groups or GFP-infected controls (Figure 4F). We next looked for any changes in learned fear memory. In each infected cohort, Gq and GFP, CNO and VEH trials consisted of separate groups to control for learned behaviors. We observed no changes between infection or treatment groups during the training or context trials (Figures 4G and 4H). However, increasing PC activity in RCrus1 significantly increased cued fear learning (Figure 4I), akin to the improvement observed upon specific expression of *Fmr1* in PCs (Figure 3J). We also tested the Gq- and GFP-infected groups in rotarod, elevated plus maze, and open field. No changes in anxiety-like behaviors or locomotor activity were observed following administration of CNO or VEH in any of the groups (Figures S5A–S5E). Taken together, these data point to improvement in social behaviors, sensory hyper-responsiveness, and associative learning in constitutive *Fmr1* mutants upon targeted chemogenetic modulation of RCrus1 PCs.

Impact of increasing excitability in LCrus1 PCs in global *Fmr1* cON mutants

To investigate whether changes in behavior resulting from cerebellar modulation in *Fmr1* cON-null mutants are specific to RCrus1, we also targeted left crus1 (LCrus1) with excitatory DREADDs and evaluated for any changes in behaviors. In prior work, we have observed that chemogenetic inhibition of LCrus1 did not result in the same behavioral deficits as observed with RCrus1 inhibition; however, we have not previously studied whether modulation of LCrus1 might also be sufficient to impact behaviors in *Fmr1* cON-null mutants.[24] We successfully targeted LCrus1 PCs in our global *Fmr1* mutants using AAV8-CaMKIIα-hM3D(Gq)-mCherry as shown above with RCrus1 (Figure S6A). Following recovery time, we evaluated behaviors starting at 6 weeks of age with CNO or VEH administration 30 min prior to behavior testing. We found that LCrus1 activation in this model elicited increased interest in a novel animal as compared to a novel object in a social approach assay following CNO administration; however, that effect was not observed in the accompanying social novelty task (Figures S6B and S6C). Social olfactory testing similarly revealed no significant changes following LCrus1 activation (Figure S6D). We tested for repetitive grooming and restricted learning in the water Y maze and subsequently did not observe any behavioral changes in either test (Figures S6E and S6F). Further tests of fear memory using fear conditioning did not yield any significant results (Figures S6G–S6I). In each learning task, the CNO and VEH trials consisted of separate groups to control for learned behaviors. Lastly, to examine whether anxiogenic or impaired motor behaviors were present, we tested these mice on the elevated plus maze and open field but observed no significant changes between groups (Figures S6J–S6M). Ultimately, LCrus1 activation does appear sufficient to impact social approach behaviors in *Fmr1* cON-null mutants. Otherwise, however, unlike what is observed with RCrus1 modulation, altering excitability in LCrus1 does not appear to significantly impact learning, repetitive, motor, or anxiety-related behaviors in *Fmr1* global mutant mice.

Cerebellar *Fmr1* improves LPAC hyperexcitability

Lastly, we sought to better understand how cerebellar changes might be resulting in behavioral improvement even in global *Fmr1* mutants. Previous studies have identified cortical hyperexcitability as a causal factor to behavioral changes in FXS,[8,9,12,13] and cerebellar connections to the cerebral cortex have been identified and associated with these behaviors.[59] We have previously demonstrated that chemogenetic stimulation of RCrus1 results in decreased activity in the contralateral/left parietal association cortex (LPAC),[24] a region whose connectivity with RCrus1 is disrupted in children with ASD and a region that is itself implicated in ASD behaviors.[24] Thus, we hypothesized that normalization of cerebellar function as seen in cON-PC mice would be sufficient to reduce cortical hyperexcitability in these global *Fmr1* mutants. Since we have shown previously that chemogenetic manipulation reduces LPAC activity, we sought to ask whether genetic expression of *Fmr1* in PCs would similarly reduce cerebral cortical activity. We again examined LPAC activity in layer 4 (Figure 5A) and identified increased firing in global *Fmr1* mutants as compared to both cON-wild-type and cON-PC cohorts (Figure 5A). Upon quantification of multi- and single-unit frequencies (Figures 5B and 5C), we similarly observed an increase in frequency for both multi- and single units in cON-null mice cortex when compared to cON-wild-type cohorts, an increase that is significantly reduced in global

mutant mice expressing *Fmr1* in PCs (cON-PCs). Taken together, these data point to a functional cerebellar-cortical connection and a reduction in cortical activity with expression of *Fmr1* in PCs, even in an otherwise global *Fmr1* mutant background.

DISCUSSION

The cerebellum has been implicated in ASD in numerous human and animal studies. However, the potential contributions and underlying mechanisms of these contributions to ASD-relevant phenotypes in FXS are not well known. We have demonstrated that cerebellar *fmr1* is necessary for the regulation of multiple ASD-relevant behaviors, with loss of *fmr1* in PCs leading to intrinsic cerebellar dysfunction, impairments in social behaviors, cognitive inflexibility, and hypersensitivity to auditory sensory stimuli. This study further points to potential translationally relevant contributions of the cerebellum, as cerebellar modulation can improve behaviors not only in cerebellar-specific models but also in global models that thus more closely imitate the condition in humans. First, constitutive mutants demonstrate deficits in social, sensory hypersensitivity, and associative learning; however, mice with *fmr1* expression in PCs do not display these phenotypes, even despite otherwise constitutive loss of *fmr1* outside of cerebellar PCs. Moreover, targeted chemogenetic stimulation of PCs in RCrus1 results in improved behaviors, not just in cerebellar *fmr1* mutants but also in constitutive/global mutants. We also hypothesized and here show evidence to support that expression of *fmr1* in PCs in an otherwise *fmr1* mutant background results in improvement in cerebral cortical hyperexcitability, consistent with previous studies showing the same impact from chemogenetic modulation of RCrus1.[24,59] Correction of cortical hyperexcitability has been associated with improvement in *fmr1* mutants, and thus cerebellar expression and cerebellar modulation may impact behaviors through this mechanism.[60,61]

Although many behavioral findings in mutants with PC-specific loss of *fmr1* are observed also in global *fmr1* mutants, the phenotypes of the two models are not identical. For instance, in water Y-maze testing, *fmr1*cOFF-PC mutants display reversal learning deficits, while no differences are observed in cON mutants. This could relate to compensation in circuits in global mutants that have not expressed *fmr1* in any tissues throughout development compared to PC *fmr1* loss but with otherwise globally retained expression in cOFF-PC mutants. In addition, differences are seen in auditory sensory testing. Global sensory hypersensitivity is common across ASD and FXS. Previous studies have provided evidence for both lateral and medial cerebellar output nuclei involvement in sensory auditory processing,[54,62] and auditory hypersensitivity is common in individuals with FXS.[36,37] Although we have previously demonstrated roles for the cerebellum and specifically RCrus1 in the regulation of social behaviors, we now demonstrate a cerebellar contribution to auditory sensitivity. Prior work has shown that inferior colliculus *fmr1* is necessary for normal responses to auditory stimuli in AGS testing.[42] Here, we show that PC *fmr1* is not necessary for normal responses to AGS stimuli but instead is sufficient to improve audiogenic hypersensitivity in global *fmr1* mutants. However, interestingly, our data point to both necessity and sufficiency for auditory startle. Whether these differences reflect different circuit mechanisms governing startle vs. AGS testing and/or whether this relates to differential connections to the inferior colliculus or to collicular-regulated networks will be an important avenue of further study. These data also potentially point to a potential

mechanism by which the cerebellum acts to modulate a cerebral cortical region with known roles in sensory processing, the LPAC. Our data reveal that cerebellar function may not be necessary to drive normal sensory function; however, cerebellar activation is sufficient to alleviate elevated responses in acoustic startle and AGS assays as well as downstream hyperexcitability in the LPAC. Evidence from individuals with FXS suggests that these aberrant responses to sensory stimuli result from an imbalance of excitation/inhibition in cortical regions.[11,63,64] Similar findings have been observed in individuals with ASD[65] following evaluations of EEG[66] and fMRI[67] data, and attempts at correcting the imbalance using approaches such as transcranial magnetic stimulation (TMS) are being studied.[68] Similarly, investigations into circuit properties in ASD animal models−including FXS[69]−describe disruptions in excitation/inhibitory network connectivity driven by altered GABA signaling.[70,71] GABA receptors are prominent in the cerebellum and are decreased in postmortem studies in ASD.[72] Loss of GABAergic inputs from the cerebellum in addition to disruptions in GABA signaling in the cortex may provide an important contributing factor to cortical hyperexcitability in FXS and other neurodevelopmental disorders, as evidenced by the reduction in hyperexcitability observed upon PC *fmr1* expression in global *fmr1* mutants. In our FXS models, we have found decreased PC function and increased single-unit frequency in the LPAC; however, with normalized PC function in our cON-PC model, we see the heightened LPAC activity return to wild-type levels. These findings not only further underscore the known connectivity between the cerebellum and ASD-related cortical areas but highlight a potential mechanism by which leveraging cerebellar mechanisms may ultimately impact disordered behavior such as social behaviors with brain-wide network contributions.

In this study, we are able to successfully ameliorate complex behavior challenges known to involve coordination of multiple cortical and subcortical regions through genetic and chemogenetic manipulations targeted to the cerebellum.[11,73–75] Our past and present results continue to support the existence of a cerebellar contribution to neuronal activity in known social and sensory implicated cortical regions, such as the median prefrontal cortex (mPFC) and LPAC.[24,59] However, mechanistically, beyond regulation of excitability, how these disruptions occur and drive broad behavioral challenges requires further characterization. The execution of complex social behaviors also involves network activation across multiple cortical areas. Ours and other studies have identified functional cerebellar connectivity to brain regions with known roles in social behavior such as the mPFC and the inferior parietal lobule (IPL) in social cognition.[24,54,59,76–79] Cerebellar regulation of social behaviors may be driven by the ability of the cerebellum to generate internal models, and evidence of this phenomenon has been observed in motor and sensory contexts.[80–83] In addition, cerebellar connections to subcortical domains including those involved in reward may provide important contributions to social behaviors.[84,85] Moreover, beyond disruptions in cerebellar-cortical communication, changes in cerebellar function may impact neuronal communication between other brain regions as well, evidence of which has been shown between the cerebellum and cerebral motor and non-motor areas such as the mPFC and hippocampus.[86–88] Whether these mechanisms underlie cerebellar modulation of precise cortical and subcortical networks involved in ASD-relevant behaviors requires further investigation.

We have demonstrated that cerebellar activation, whether through genetic manipulation or chemogenetic targeting of a precise cerebellar domain, is sufficient to impact altered behaviors that resulted from PC-specific genetic mutations and in a more translationally relevant global genetic mutant.[24,59] Moreover, the impact of increasing excitability has at least some specificity, with chemogenetic modulation of RCrus1 impacting different behaviors than behavioral changes observed with LCrus1. Taken together, these data point to lateralization within the cerebellum that impacts the sufficiency of Crus1 modulation to impact behaviors, which adds to prior data pointing to lateralization in Crus1's necessity for regulation of ASD-relevant behaviors.[24,59] It is worth noting that although these data point to important roles for Crus1, further studies examining whether other cerebellar domains might also be sufficient to improve relevant behaviors remain critical avenues for further study. In combination with further elaboration of the circuit networks connecting to Crus1, these studies may provide opportunities to leverage those discoveries for the development of targeted therapeutics for individuals with neurodevelopmental disorders who are seeking therapeutic options.

Together, our findings identify a role for the cerebellum in regulating ASD-relevant behaviors in FXS. This dataset, combined with previous studies, confirms a cerebellar contribution to multiple models of genetic ASD and that improvement of impaired social behaviors, driven by translationally relevant whole-brain loss of *fmr1*, can be achieved with specific genetic or chemogenetic manipulation of the cerebellum. Further investigation into the functional mechanisms of this beneficial modulation, the necessary study in both sexes, the potential shared translational mechanisms, and impacts in individuals with FXS will be important avenues of future study.

Limitations of the study

Our data show that cerebellar *fmr1* plays important roles in the regulation of ASD-relevant behaviors. Moreover, our data further support that modulation of cerebellar region RCrus1 is sufficient to ameliorate these behaviors in both cerebellar and global *fmr1* mutant models. These data, however, will not fully characterize the topography of the cerebellar contribution to these behaviors. Whether additional regions within the cerebellum contribute to these behaviors will be an important avenue of future studies. Moreover, we also demonstrate that RCrus1 modulation demonstrates different ability to impact behaviors when compared to LCrus1. The mechanisms underlying these differences in laterality will similarly be critical directions of future study. Moreover, these studies have focused on the cerebellar contributions and have highlighted alterations from cerebellar changes on cerebral cortical activity. It will be critical to better understand the extent of the impact of these cerebellar changes on brain-wide functions and to show how and which changes have important contributions that are relevant to these neurodevelopmental behaviors. In addition, these studies have been limited to male cohorts, as FXS predominantly impacts males; however, potential sex differences in these phenotypes are an important gap in knowledge and will be an important direction for future study. Lastly, whether these findings are applicable to individuals with FXS and other neurodevelopmental challenges remains to be determined. The potential translational implication of these findings remains an open question and an important limitation, all of which will be critical future directions of additional study.

STAR★METHODS

RESOURCE AVAILABILITY

Lead contact—Further information and requests for resources and reagents should be directed to and will be fulfilled by the lead contact, Peter Tsai (Peter.Tsai@utsouthwestern.edu).

Materials availability—This study did not generate any unique reagents.

Data and code availability

- All data reported in this paper will be shared by the lead contact upon request.
- All code can be found on github: https://doi.org/10.5281/zenodo.10092944 (https://doi.org/10.5281/zenodo.10092944)
- Any additional information required to re-analyze the data reported in this paper will be available from the lead contact upon request.

EXPERIMENTAL MODEL AND STUDY PARTICIPANT DETAILS

To generate the Purkinje cell conditional OFF (cOFF) mouse lines (cOFF-PC and cOFF-Control), *L7/Pcp2-Cre (L7^{Cre})* transgenic mice were obtained from Jackson Laboratories (004146) and crossed with *Fmr1*$^{flox/flox}$ female mice. *Fmr1*$^{flox/flox}$ mice were generously provided by Dr. David Nelson, (Baylor College of Medicine, Houston, TX). This generated L7^{Cre+};*Fmr1*$^{flox/flox}$ females *and L7*$^{Cre+}$;*Fmr1*$^{flox/y}$ males. *L7*$^{Cre+}$;*Fmr1*$^{flox/flox}$ females were crossed to *L7*$^{Cre-}$;*Fmr1*$^{flox/y}$ males to generate and maintain the colony. *L7*$^{Cre-}$;*Fmr1*$^{flox/y}$ and *L7*$^{Cre+}$;*Fmr1*$^{flox/y}$ males were used for all experiments. Using the *loxP* system, *Fmr1* is deleted from PCs using the *L7*^{Cre}. Of note, previous studies have additionally shown some Cre expression in retinal cells, a few cerebellar molecular layer interneurons, and a small number of cells distributed across the brain using this specific Cre line.[20,90]

To generate the Purkinje cell conditional ON (cON) lines (cON-null, cON-PC, and cON-Wildtype) the *L7/Pcp2-Cre (L7*^{Cre}*)* transgenic mice were crossed with *Fmr1 cON*$^{flox/flox}$ females (also generously provided by Dr. David Nelson from Baylor College of Medicine, Houston, TX). This generated *Fmr1 cON*$^{flox/+}$ females which were then crossed to the *L7/Pcp2-Cre* line to generate the following males, used for all experiments: L7^{Cre-};*Fmr1-cON*$^{flox/y}$ (cON-null), L7^{Cre+};*Fmr1-cON*$^{flox/y}$ (cON-PC), and *L7*$^{Cre+\ or-}$ *Fmr1-cON*$^{+/y}$ (cON-wildtype). Expression of the *Fmr1* gene is driven by the presence of the *L7*^{Cre}, without the *L7*^{Cre} *Fmr1* is not expressed, with it, *Fmr1* expresses properly in PCs. Both cOFF and cON lines were obtained from Dr. David Nelson (Baylor College of Medicine, Houston, TX). See Table S12.

The *Fmr1* gene is X-linked; thus FXS is more often observed in males as compared to females. As a result, only male mice were used for all behavioral and physiological testing.[91] Mice were aged 5–12 weeks and of mixed genetic backgrounds (C57Bl/6J, 129 SvJae and BALB/cJ). As littermate controls were used for all behavioral experiments, no appreciable physical characteristics (e.g., weight, size, coat color) should impact blinding

of examiners. The University of Texas Southwestern Institutional Animal Care and Use Committees approved all experimental protocols in this study.

METHOD DETAILS

Stereotaxic viral injections—Viral vectors used in behavioral experiments were delivered to cerebellar RCrus1 with a nanoinjector (WPI) under stereotaxic guidance (Stoelting) in mice anesthetized with a mix of ketamine (100 mg/kg) and xylazine (10 mg/kg). 400nL of AAV8-CamKIIa-hM3D(Gq)-mCherry or AAV8-CamKIIa-GFP were used for viral injections. All viruses were purchased from Addgene. Location of RCrus1 injections from bregma (*x*, *y*, *z*), −2.5, −6.36, −2.5.

Chemogenetic activation—Clozapine -N- Oxide (CNO) was purchased from Tocris Bioscience and reconstituted to 1 mg/mL concentration with 0.9% saline with dimethyl sulfoxide to 0.5%. Vehicle (VEH) contained 0.9% saline with DMSO to 0.5%. Mice were injected intraperitoneally 30 min prior to behavioral testing with 2 mg/kg CNO or VEH.

Anesthetized *in vivo* electrophysiology—Male mice were used for *in vivo* anesthetized extracellular single- and multi-unit recordings. Recordings were performed in the left parietal association cortex (LPAC).[24] Mice were anesthetized with a ketamine (100 mg/kg) and xylazine (10 mg/kg) mix initially and placed in a stereotaxic apparatus. A craniotomy was performed to remove a small area of the skull and expose the surface of the brain at the site of recording. Forty-minutes after the first anesthetic injection, ketamine alone (100 mg/ml in saline) was administered intraperitoneally to accommodate for a shorter ketamine half-life compared to xylazine. A TC-1000 temperature controller with a rectal probe kept the mice at 37°C. Tungsten microelectrodes (World Precision Instruments; 3-μm insulation, 0.356-mm shaft, 2 MΩ, 1–2-μm tip) were inserted to layer 4 of the LPAC. The depth of insertion to layer 4 was informed by brain slice immunohistochemistry and coincided with maximal amplitude of detected multi-units. Electrophysiological activity was acquired, amplified and band-pass filtered (low-pass filter, 25 kHz; high-pass filter, 400 Hz) with a MultiClamp 700B programmable amplifier (Molecular Devices). Location for LPAC recordings: (x, y, z), −1.4, −1.9, −0.7. Data analysis was done offline using algorithms written in MATLAB. Putative multiunits were detected in a recording as amplitude deflections greater than 5 times the median absolute deviation from the baseline.[92] Wave_Clus was used for semi-automated spike sorting and clustering of single units,[92] followed by manual confirmation of single unit shape analysis to identify distinct single units. Analysis was done with a provision in the code to blind the researcher to the group designation of recordings being analyzed.

Acute slice electrophysiology—Acute sagittal slices (250–300 μm thick) were prepared from the cerebellar vermis of 8 and 12-week-old mutant and control littermates from each treatment group. Slices were cut in an ice-cold artificial cerebrospinal fluid (ACSF) solution consisting of (mM): 125 NaCl, 26 $NaHCO_3$, 1.25 NaH_2PO_4, 2.5 KCl, 1 $MgCl_2$, 2 $CaCl_2$, and 25 glucose (pH 7.3, osmolarity 310) equilibrated with 95% O_2 and 5% CO_2. Slices were initially incubated at 34°C for 25 min, and then at room temperature

(21–22°C) prior to recording in the same ACSF. For acute slice recordings CNO studies were performed at 10 μM.

Recordings—Visually guided (infrared DIC videomicroscopy and water-immersion 40× objective) whole-cell recordings were obtained with patch pipettes (2–4 MΩ) pulled from borosilicate capillary glass (World Precision Instruments) with a Sutter P-97 horizontal puller. Electrophysiological recordings were performed at 31°C–33°C. For current-clamp recordings, the internal solution contained (in mM): 150 potassium-gluconate, 3 KCl, 10 HEPES, 0.5 EGTA, 3 MgATP, 0.5 GTP, 5 phosphocreatine-tris$_2$, and 5 phosphocreatine-Na$_2$. pH was adjusted to 7.2 with NaOH. Current-clamp and extracellular recordings were performed in NBQX (5 μM) (Sigma, N183), R-CPP (2.5 μM) (Tocris, 0247), and picrotoxin (20 μM) (Tocris, 1128) to block AMPA receptors, NMDA receptors, and GABA$_A$ receptors respectively.

Data acquisition and analysis—Electrophysiological data were acquired using a Multiclamp 700B amplifier (Axon Instruments) digitized at 20 kHz with either a National Instruments USB-6229 or PCI-MIO 16E-4 board and filtered at 2 kHz. Acquisition was controlled both with custom software written in either MATLAB or pCLAMP. Series resistance was monitored in voltage-clamp recordings with a 5-mV hyperpolarizing pulse, and only recordings that remained stable over the period of data collection were used. Glass monopolar electrodes (1–2 MΩ) filled with ACSF in conjunction with a stimulus isolation unit (WPI, A360) were used for extracellular stimulation of climbing and parallel fibers.

Immunohistochemistry—Mice were perfused and post-fixed with 4% paraformaldehyde. For quantifying Purkinje cell numbers, sections were prepared by cryostat sectioning and were stained with mouse monoclonal anti-calbindin (Sigma, #C9848) to identify Purkinje cells. Quantification of Purkinje cells was completed by totaling Purkinje neurons from midline vermis sections from mice from each model.

For FMRP localization, cerebellar cryosections were bathed in boiling citrate buffer for antigen retrieval prior to co-staining with anti-FMRP 2F-5 antibody (Iowa Hybridoma) and rabbit monoclonal anti-calbindin (abcam, [EP3478] ab108404), slices were taken from mice aged 10–12 weeks.

Behavioral analysis—Statistics of behavioral experiments can be found in Tables S1–S4, S5–S10, and S11. Behavioral studies were performed with male mice, with repeat testing performed for the following behavioral tests: elevated plus maze, open field, three-chambered apparatus, grooming and olfaction, and startle testing. Mice were randomly assigned to groups for viral injection type. Each mouse performed these testing paradigms with VEH and CNO. Starting treatment was randomly assigned and then alternated between VEH and CNO treatments. To minimize previous exposure to the task, repeated testing in a specific behavioral paradigm was separated by 1 week. Testing was performed in the order listed above. For rotarod and water maze testing, which were performed in the weeks after the above testing, mice were randomly assigned to one treatment group (either VEH or CNO), and no repeat testing was performed owing to the learning component involved in these tests. Animals were group housed under a 12-h light: dark cycle. Chemogenetic studies

involved the following controls: GFP infection (VEH and CNO) and designer receptors exclusively activated by designer drugs (DREADD) infection (VEH and CNO) for all behavioral studies to control for DREADD activation and potential off-target effects of CNO off-target effects.[93] All behavioral assays were performed by examiners blinded to infection type.

Accelerating rotarod—Animals were tested using the accelerating rotarod over 5 consecutive days.[94] Latency to fall was recorded. Animals were tested between 7 and 12 weeks of age.

Open field—Open field testing was performed for a 15-min period.[95] Movement and time spent in the center quadrants were recorded by video camera and automated analysis was performed using Noldus Ethovison software version 12.5. Light at the center of the open field was 30 lux. Animals were tested between 8 and 12 weeks of age.

Elevated plus maze—Elevated plus maze testing was performed for a 5-min period.[95] Distance traveled and time in open arms was recorded by video camera and automated analysis was performed using Noldus Ethovision software version 12.5. Light in the open arms was 20 lux. Animals were tested between 8 and 12 weeks of age.

Social interaction—Animals were tested for social interaction in the three-chambered apparatus (Nationwide Plastics).[96] Animals were individually housed for 30 min before being placed in the middle chamber of the three-chambered apparatus for 10 min. Next, in the habituation phase, the animals explored the entire apparatus for 10 min. A novel animal (male, age matched, C57BL/6j) and novel object (wire cup) were then inserted into opposite chambers of the apparatus and animals were tested for 10 min in this social approach model. Then, a novel animal was inserted into the chamber in place of the novel object and social novelty was evaluated for an additional 10 min. Time spent in each chamber and the number of crossings between chambers were recorded in an automated manner (Noldus Ethovision software version 12.5). Time spent interacting with the novel animal and novel object was scored with a stopwatch by an examiner who was blinded to experimental condition and genotype. Animals were tested between 8 and 12 weeks of age. Light at the center of the three-chambered apparatus was 30 lux for all experiments.

Olfaction—Olfaction was tested using the habituation/dishabituation experimental model.[97] Animals were briefly habituated to the testing environment for 30-min, then sequentially presented with cotton swabs dipped in water, almond extract, or banana extract diluted at 1:200 (McCormick). Social olfactory stimuli were derived from cage swipes of sex-matched mice that had never come in contact with tested animals.[20,24,59,97] Mice were exposed to each olfactory stimulus for three 2-min trials. Time spent sniffing each olfactory stimulus was recorded. Animals were tested between 8 and 12 weeks of age.

Grooming—Animals were removed from home cages and placed individually into new cages containing bedding only. Animals were allowed to habituate to the new cage for 10-min. Animals were then observed for 10-min and time spent grooming was scored by an

examiner blinded to experimental condition and genotype.[98] Animals were tested between 8 and 12 weeks of age.

Water Y maze—Reversal learning was testing using the water Y maze.[99] Animals were briefly habituated to the apparatus. For the first three trial sessions, mice were given 15 trials to locate a submerged platform placed in one of the maze arms. After the third trial session, the platform was moved to the other arm of the Y maze. Mice were then tested for three additional sessions with 15 trials per session (reversal trials 1–3). Animals underwent two trial sessions per day, and the number of correct trials was recorded. Animals were tested between 9 and 13 weeks of age.

Fear conditioning—Associative fear memory was tested for three consecutive days using VideoFreeze (Med-Associates Inc., Georgia, VT, USA). On training day animals were placed in a chamber with white light for 3 min, then a tone is played paired with a foot shock (0.05mA) 3 times over the next 3 min. This tone/shock pairing occurs once every minute, once the test is complete the animal is returned to their home cage. 24 h later, context day, the animal is placed back in the chamber for 5 min with the white light but no tone or shock and is returned to their home cage after. For cued testing, the chamber is altered to appear as a “new environment”: the white light remains present, but the walls and floor are covered with plastic and vanilla extract is placed underneath the chamber floor. Animals are placed in the new environment for 3 min, then the tone from training day is played for the duration of the next 3 min. The amount of time the animal spends freezing is recorded. Animals were tested between 10 and 13 weeks of age.

Acoustic startle—Acoustic startle reflex is tested in one session. The animal is placed into a small plastic tube attached to a base that monitors movement. After habituating to the tube for 5 min, animals are exposed to bursts of white noise at 80dB, 90dB, 100dB, 110dB or 120dB in random sequence for 8 trials. A “no stimulus” condition was included in each trial to measure baseline movement. The amplitude of the startle response for each mouse is recorded using SR-Lab System (San Diego Instruments, San Diego, CA, USA).

Audiogenic seizures—AGSs were induced in mice between P18-P24.[100,101] Mice were placed in a plastic chamber (30 × 19 × 12 cm) containing a door alarm (GE 50246 personal security alarm) and covered with a plastic lid. A 120 dB siren sound was presented to mice for 3 min. Mice were scored for behavioral phenotype based on experimenter observation, as follows: 0 = no response; 1 = wild running; 2 = tonic-clonic seizures; 3 = status epilepticus/death. As AGS is performed only during this early time period, AGS was not tested in cON-null – Crus1 chemogenetic experiments which were performed during adulthood to facilitate recovery from the intracranial injection.

QUANTIFICATION AND STATISTICAL ANALYSIS

Statistics data are reported as a mean ± SEM, and statistical analysis was carried out with GraphPad Prism software using two-way ANOVA with Bonferroni’s multiple comparison tests for post hoc analysis. Significance was defined as $p < 0.05$. Number of animals and statistical results utilized for all studies is included in Tables S1–S4, S5–S10, and S11.

ROUT methodology in GraphPad Prism was utilized to determine the presence of outliers with highest stringency threshold of q = 0.1%.

Supplementary Material

Refer to Web version on PubMed Central for supplementary material.

ACKNOWLEDGMENTS

We would like to thank the University of Texas Southwestern Medical Center Whole Brain Microscopy Core Facility, RRID:SCR_017949, for aid with microscopy and imaging. We also thank the University of Texas Southwestern Medical Center Behavioral Phenotyping Core and Shari Birnbaum for assistance with behavioral phenotyping studies. We also thank Dr. David Nelson for his generous sharing of multiple *Fmr1* models (*Fmr1 cOFF*; *Fmr1 cON*) utilized in this study. We would also like to acknowledge Drs. Kim Huber, Helen Lai, and Genevieve Konopka and members of the Tsai lab for feedback on experiments and manuscript edits. P.T.T. was supported by the National Institute of Neurologic Disorders and Stroke of the National Institutes of Health (NIH) grant K08 NS083733 and the National Institute of Mental Health of the NIH grants R01 MH116882 and R01 MH120069-01A1. J.M.G. was supported by the National Heart, Lung, and Blood Institute grant 1T32HL139438-01A1 and the Sleep and Circadian Rhythms Training Program grant T32HL139438. J.M.P. was supported by the National Institute of Neurological Disorders and Stroke grants NS102588 and NS077015.

REFERENCES

1. SFARI Gene Database (2022). Human Gene Module.
2. Rosenberg RE, Law JK, Yenokyan G, McGready J, Kaufmann WE, and Law PA (2009). Characteristics and concordance of autism spectrum disorders among 277 twin pairs. Arch. Pediatr. Adolesc. Med. 163, 907–914. [PubMed: 19805709]
3. Abrahams BS, and Geschwind DH (2008). Advances in autism genetics: on the threshold of a new neurobiology. Nat. Rev. Genet. 9, 341–355. [PubMed: 18414403]
4. Ramaswami G, and Geschwind DH (2018). Genetics of autism spectrum disorder. Handb. Clin. Neurol. 147, 321–329. [PubMed: 29325621]
5. Tassone F, Hagerman RJ, Chamberlain WD, and Hagerman PJ (2000). Transcription of the FMR1 gene in individuals with fragile X syndrome. Am. J. Med. Genet. 97, 195–203. [PubMed: 11449488]
6. Hagerman R, Hoem G, and Hagerman P. (2010). Fragile X and autism: Intertwined at the molecular level leading to targeted treatments. Mol. Autism. 1, 12. [PubMed: 20858229]
7. Bailey DB Jr., Raspa M, Olmsted M, and Holiday DB (2008). Co-occurring conditions associated with FMR1 gene variations: findings from a national parent survey. Am. J. Med. Genet. 146a, 2060–2069. [PubMed: 18570292]
8. Huber KM, Gallagher SM, Warren ST, and Bear MF (2002). Altered synaptic plasticity in a mouse model of fragile X mental retardation. Proc. Natl. Acad. Sci. USA 99, 7746–7750. [PubMed: 12032354]
9. Bear MF, Huber KM, and Warren ST (2004). The mGluR theory of fragile X mental retardation. Trends Neurosci. 27, 370–377. [PubMed: 15219735]
10. Guo W, Allan AM, Zong R, Zhang L, Johnson EB, Schaller EG, Murthy AC, Goggin SL, Eisch AJ, Oostra BA, et al. (2011). Ablation of Fmrp in adult neural stem cells disrupts hippocampus-dependent learning. Nat. Med. 17, 559–565. [PubMed: 21516088]
11. Wang J, Ethridge LE, Mosconi MW, White SP, Binder DK, Pedapati EV, Erickson CA, Byerly MJ, and Sweeney JA (2017). A resting EEG study of neocortical hyperexcitability and altered functional connectivity in fragile X syndrome. J. Neurodev. Disord. 9, 11. [PubMed: 28316753]
12. Gibson JR, Bartley AF, Hays SA, and Huber KM (2008). Imbalance of neocortical excitation and inhibition and altered UP states reflect network hyperexcitability in the mouse model of fragile X syndrome. J. Neurophysiol. 100, 2615–2626. [PubMed: 18784272]
13. Gonç alves JT, Anstey JE, Golshani P, and Portera-Cailliau C. (2013). Circuit level defects in the developing neocortex of Fragile X mice. Nat. Neurosci. 16, 903–909. [PubMed: 23727819]

14. Bauman M, and Kemper TL (1985). Histoanatomic observations of the brain in early infantile autism. Neurology 35, 866–874. [PubMed: 4000488]
15. Whitney ER, Kemper TL, Bauman ML, Rosene DL, and Blatt GJ (2008). Cerebellar Purkinje cells are reduced in a subpopulation of autistic brains: a stereological experiment using calbindin-D28k. Cerebellum 7, 406–416. [PubMed: 18587625]
16. Greco CM, Navarro CS, Hunsaker MR, Maezawa I, Shuler JF, Tassone F, Delany M, Au JW, Berman RF, Jin LW, et al. (2011). Neuropathologic features in the hippocampus and cerebellum of three older men with fragile X syndrome. Mol. Autism. 2, 2. [PubMed: 21303513]
17. Ellegood J, Pacey LK, Hampson DR, Lerch JP, and Henkelman RM (2010). Anatomical phenotyping in a mouse model of fragile X syndrome with magnetic resonance imaging. Neuroimage 53, 1023–1029. [PubMed: 20304074]
18. Ellegood J, and Crawley JN (2015). Behavioral and Neuroanatomical Phenotypes in Mouse Models of Autism. Neurotherapeutics 12, 521–533. [PubMed: 26036957]
19. D'Mello AM, and Stoodley CJ (2015). Cerebro-cerebellar circuits in autism spectrum disorder. Front. Neurosci. 9, 408. [PubMed: 26594140]
20. Tsai PT, Hull C, Chu Y, Greene-Colozzi E, Sadowski AR, Leech JM, Steinberg J, Crawley JN, Regehr WG, and Sahin M. (2012). Autistic-like behaviour and cerebellar dysfunction in Purkinje cell Tsc1 mutant mice. Nature 488, 647–651. [PubMed: 22763451]
21. Peter S, ten Brinke MM, Stedehouder J, Reinelt CM, Wu B, Zhou H, Zhou K, Boele H-J, Kushner SA, Lee MG, et al. (2016). Dysfunctional cerebellar Purkinje cells contribute to autism-like behaviour in Shank2-deficient mice. Nat. Commun. 7, 12627. [PubMed: 27581745]
22. Reith RM, McKenna J, Wu H, Hashmi SS, Cho S-H, Dash PK, and Gambello MJ (2013). Loss of Tsc2 in Purkinje cells is associated with autistic-like behavior in a mouse model of tuberous sclerosis complex. Neurobiol. Dis. 51, 93–103. [PubMed: 23123587]
23. Cupolillo D, Hoxha E, Faralli A, De Luca A, Rossi F, Tempia F, and Carulli D. (2016). Autistic-Like Traits and Cerebellar Dysfunction in Purkinje Cell PTEN Knock-Out Mice. Neuropsychopharmacology 41, 1457–1466. [PubMed: 26538449]
24. Stoodley CJ, D'Mello AM, Ellegood J, Jakkamsetti V, Liu P, Nebel MB, Gibson JM, Kelly E, Meng F, Cano CA, et al. (2017). Altered cerebellar connectivity in autism and cerebellar-mediated rescue of autism-related behaviors in mice. Nat. Neurosci. 20, 1744–1751. [PubMed: 29184200]
25. Heck DH, Zhao Y, Roy S, LeDoux MS, and Reiter LT (2008). Analysis of cerebellar function in Ube3a-deficient mice reveals novel genotype-specific behaviors. Hum. Mol. Genet. 17, 2181–2189. [PubMed: 18413322]
26. Kamath SP, and Chen AI (2019). Myocyte Enhancer Factor 2c Regulates Dendritic Complexity and Connectivity of Cerebellar Purkinje Cells. Mol. Neurobiol. 56, 4102–4119. [PubMed: 30276662]
27. Kloth AD, Badura A, Li A, Cherskov A, Connolly SG, Giovannucci A, Bangash MA, Grasselli G, Peñagarikano O, Piochon C, et al. (2015). Cerebellar associative sensory learning defects in five mouse autism models. Elife 4, e06085.
28. Piochon C, Kloth AD, Grasselli G, Titley HK, Nakayama H, Hashimoto K, Wan V, Simmons DH, Eissa T, Nakatani J, et al. (2014). Cerebellar plasticity and motor learning deficits in a copy-number variation mouse model of autism. Nat. Commun. 5, 5586. [PubMed: 25418414]
29. Loesch DZ, Litewka L, Brotchie P, Huggins RM, Tassone F, and Cook M. (2005). Magnetic resonance imaging study in older fragile X premutation male carriers. Ann. Neurol. 58, 326–330. [PubMed: 16049924]
30. Moore CJ, Daly EM, Tassone F, Tysoe C, Schmitz N, Ng V, Chitnis X, McGuire P, Suckling J, Davies KE, et al. (2004). The effect of pre-mutation of X chromosome CGG trinucleotide repeats on brain anatomy. Brain 127, 2672–2681. [PubMed: 15483045]
31. Koekkoek SKE, Yamaguchi K, Milojkovic BA, Dortland BR, Ruigrok TJH, Maex R, De Graaf W, Smit AE, VanderWerf F, Bakker CE, et al. (2005). Deletion of FMR1 in Purkinje Cells Enhances Parallel Fiber LTD, Enlarges Spines, and Attenuates Cerebellar Eyelid Conditioning in Fragile X Syndrome. Neuron 47, 339–352. [PubMed: 16055059]
32. Yang Y-M, Arsenault J, Bah A, Krzeminski M, Fekete A, Chao OY, Pacey LK, Wang A, Forman-Kay J, Hampson DR, and Wang L-Y (2020). Identification of a molecular locus for normalizing

dysregulated GABA release from interneurons in the Fragile X brain. Mol. Psychiatr. 25, 2017–2035.

33. Khandjian EW, Fortin A, Thibodeau A, Tremblay S, Côté F, Devys D, Mandel JL, and Rousseau F. (1995). A heterogeneous set of FMR1 proteins is widely distributed in mouse tissues and is modulated in cell culture. Hum. Mol. Genet. 4, 783–789. [PubMed: 7633436]
34. Barski JJ, Dethleffsen K, and Meyer M. (2000). Cre recombinase expression in cerebellar Purkinje cells. Genesis 28, 93–98. [PubMed: 11105049]
35. Richler J, Huerta M, Bishop SL, and Lord C. (2010). Developmental trajectories of restricted and repetitive behaviors and interests in children with autism spectrum disorders. Dev. Psychopathol. 22, 55–69. [PubMed: 20102647]
36. Rojas DC, Benkers TL, Rogers SJ, Teale PD, Reite ML, and Hagerman RJ (2001). Auditory evoked magnetic fields in adults with fragile X syndrome. Neuroreport 12, 2573–2576. [PubMed: 11496151]
37. Van der Molen MJW, Van der Molen MW, Ridderinkhof KR, Hamel BCJ, Curfs LMG, and Ramakers GJA (2012). Auditory and visual cortical activity during selective attention in fragile X syndrome: A cascade of processing deficiencies. Clin. Neurophysiol. 123, 720–729. [PubMed: 21958658]
38. Rais M, Binder DK, Razak KA, and Ethell IM (2018). Sensory Processing Phenotypes in Fragile X Syndrome. ASN neuro 10, 1759091418801092.
39. Rotschafer SE, and Razak KA (2014). Auditory processing in fragile x syndrome. Front. Cell. Neurosci. 8, 19. [PubMed: 24550778]
40. Musumeci SA, Bosco P, Calabrese G, Bakker C, De Sarro GB, Elia M, Ferri R, and Oostra BA (2000). Audiogenic Seizures Susceptibility in Transgenic Mice with Fragile X Syndrome. Epilepsia 41, 19–23. [PubMed: 10643918]
41. Sawicka K, Pyronneau A, Chao M, Bennett MVL, and Zukin RS (2016). Elevated ERK/p90 ribosomal S6 kinase activity underlies audiogenic seizure susceptibility in fragile X mice. Proc. Natl. Acad. Sci. USA 113. E6290–e6297. [PubMed: 27663742]
42. Gonzalez D, Tomasek M, Hays S, Sridhar V, Ammanuel S, Chang C. w., Pawlowski K, Huber KM, and Gibson JR (2019). Audiogenic Seizures in the Fmr1 Knock-Out Mouse Are Induced by Fmr1 Deletion in Subcortical, VGlut2-Expressing Excitatory Neurons and Require Deletion in the Inferior Colliculus. J. Neurosci. 39, 9852–9863. [PubMed: 31666356]
43. Hessl D, Rivera S, Koldewyn K, Cordeiro L, Adams J, Tassone F, Hagerman PJ, and Hagerman RJ (2007). Amygdala dysfunction in men with the fragile X premutation. Brain 130, 404–416. [PubMed: 17166860]
44. Fernandes G, Mishra PK, Nawaz MS, Donlin-Asp PG, Rahman MM, Hazra A, Kedia S, Kayenaat A, Songara D, Wyllie DJA, et al. (2021). Correction of amygdalar dysfunction in a rat model of fragile X syndrome. Cell Rep. 37, 109805.
45. Sacchetti B, Baldi E, Lorenzini CA, and Bucherelli C. (2002). Cerebellar role in fear-conditioning consolidation. Proc. Natl. Acad. Sci. USA 99, 8406–8411. [PubMed: 12034877]
46. Medina JF, Nores WL, Ohyama T, and Mauk MD (2000). Mechanisms of cerebellar learning suggested by eyelid conditioning. Curr. Opin. Neurobiol. 10, 717–724. [PubMed: 11240280]
47. Albergaria C, Silva NT, Pritchett DL, and Carey MR (2018). Locomotor activity modulates associative learning in mouse cerebellum. Nat. Neurosci. 21, 725–735. [PubMed: 29662214]
48. Bauman ML (2010). Medical comorbidities in autism: Challenges to diagnosis and treatment. Neurotherapeutics 7, 320–327. [PubMed: 20643385]
49. Amaral DG, Schumann CM, and Nordahl CW (2008). Neuroanatomy of autism. Trends Neurosci. 31, 137–145. [PubMed: 18258309]
50. Cupolillo D, Hoxha E, Faralli A, De Luca A, Rossi F, Tempia F, and Carulli D. (2016). Autistic-Like Traits and Cerebellar Dysfunction in Purkinje Cell PTEN Knock-Out Mice. Neuropsychopharmacology 41, 1457–1466. [PubMed: 26538449]
51. Steadman PE, Ellegood J, Szulc KU, Turnbull DH, Joyner AL, Henkelman RM, and Lerch JP (2014). Genetic effects on cerebellar structure across mouse models of autism using a magnetic resonance imaging atlas. Autism Res. 7, 124–137. [PubMed: 24151012]

52. Takarae Y, Minshew NJ, Luna B, and Sweeney JA (2007). Atypical involvement of frontostriatal systems during sensorimotor control in autism. Psychiatr. Res. 156, 117–127.
53. Allen G, Müller RA, and Courchesne E. (2004). Cerebellar function in autism: Functional magnetic resonance image activation during a simple motor task. Biol. Psychiatr. 56, 269–278.
54. Stoodley CJ, and Schmahmann JD (2009). Functional topography in the human cerebellum: A meta-analysis of neuroimaging studies. Neuroimage 44, 489–501. [PubMed: 18835452]
55. Spencer CM, Alekseyenko O, Serysheva E, Yuva-Paylor LA, and Paylor R. (2005). Altered anxiety-related and social behaviors in the Fmr1 knockout mouse model of fragile X syndrome. Gene Brain Behav. 4, 420–430.
56. Bakker C, Verheij C, Willemsen R, Van Der Helm R, and Oerlemans F. (1994). Fmr1 knockout mice: a model to study fragile X mental retardation. Cell 78, 23–33. [PubMed: 8033209]
57. Curia G, Gualtieri F, Bartolomeo R, Vezzali R, and Biagini G. (2013). Resilience to audiogenic seizures is associated with p-ERK1/2 dephosphorylation in the subiculum of Fmr1 knockout mice. Front. Cell. Neurosci. 7, 46. [PubMed: 23630463]
58. Olmos-Serrano JL, and Corbin JG (2011). Amygdala regulation of fear and emotionality in fragile X syndrome. Dev. Neurosci. 33, 365–378. [PubMed: 21893939]
59. Kelly E, Meng F, Fujita H, Morgado F, Kazemi Y, Rice LC, Ren C, Escamilla CO, Gibson JM, Sajadi S, et al. (2020). Regulation of autism-relevant behaviors by cerebellar–prefrontal cortical circuits. Nat. Neurosci. 23, 1102–1110. [PubMed: 32661395]
60. Hays SA, Huber KM, and Gibson JR (2011). Altered neocortical rhythmic activity states in Fmr1 KO mice are due to enhanced mGluR5 signaling and involve changes in excitatory circuitry. J. Neurosci. 31, 14223–14234. [PubMed: 21976507]
61. Hébert B, Pietropaolo S, Même S, Laudier B, Laugeray A, Doisne N, Quartier A, Lefeuvre S, Got L, Cahard D, et al. (2014). Rescue of fragile X syndrome phenotypes in Fmr1 KO mice by a BKCa channel opener molecule. Orphanet J. Rare Dis. 9, 124. [PubMed: 25079250]
62. Keren-Happuch E, Chen SHA, Ho MHR, and Desmond JE (2014). A meta-analysis of cerebellar contributions to higher cognition from PET and fMRI studies. Hum. Brain Mapp. 35, 593–615. [PubMed: 23125108]
63. Ferri R, Musumeci SA, Elia M, Del Gracco S, Scuderi C, and Bergonzi P. (1994). BIT-mapped somatosensory evoked potentials in the fragile X syndrome. Neurophysiologie Clinique/Clinical Neurophysiology 24, 413–426. [PubMed: 7723725]
64. Ethridge LE, White SP, Mosconi MW, Wang J, Byerly MJ, and Sweeney JA (2016). Reduced habituation of auditory evoked potentials indicate cortical hyper-excitability in Fragile X Syndrome. Transl. Psychiatry 6, e787. [PubMed: 27093069]
65. Rubenstein JLR, and Merzenich MM (2003). Model of autism: increased ratio of excitation/inhibition in key neural systems. Gene Brain Behav. 2, 255–267.
66. Wang J, Barstein J, Ethridge LE, Mosconi MW, Takarae Y, and Sweeney JA (2013). Resting state EEG abnormalities in autism spectrum disorders. J. Neurodev. Disord. 5, 24. [PubMed: 24040879]
67. Haigh SM, Heeger DJ, Dinstein I, Minshew N, and Behrmann M. (2015). Cortical variability in the sensory-evoked response in autism. J. Autism Dev. Disord. 45, 1176–1190. [PubMed: 25326820]
68. Uzunova G, Pallanti S, and Hollander E. (2016). Excitatory/inhibitory imbalance in autism spectrum disorders: Implications for interventions and therapeutics. World J. Biol. Psychiatr. 17, 174–186.
69. Selby L, Zhang C, and Sun QQ (2007). Major defects in neocortical GABAergic inhibitory circuits in mice lacking the fragile X mental retardation protein. Neurosci. Lett. 412, 227–232. [PubMed: 17197085]
70. Chao HT, Chen H, Samaco RC, Xue M, Chahrour M, Yoo J, Neul JL, Gong S, Lu HC, Heintz N, et al. (2010). Dysfunction in GABA signalling mediates autism-like stereotypies and Rett syndrome phenotypes. Nature 468, 263–269. [PubMed: 21068835]
71. Tabuchi K, Blundell J, Etherton MR, Hammer RE, Liu X, Powell CM, and Südhof TC (2007). A neuroligin-3 mutation implicated in autism increases inhibitory synaptic transmission in mice. Science 318, 71–76. [PubMed: 17823315]
72. Fatemi SH, Folsom TD, Reutiman TJ, and Thuras PD (2009). Expression of GABA(B) receptors is altered in brains of subjects with autism. Cerebellum 8, 64–69. [PubMed: 19002745]

73. Golden CE, Buxbaum JD, and De Rubeis S. (2018). Disrupted circuits in mouse models of autism spectrum disorder and intellectual disability. Curr. Opin. Neurobiol. 48, 106–112. [PubMed: 29222989]
74. Contractor A, Klyachko VA, and Portera-Cailliau C. (2015). Altered Neuronal and Circuit Excitability in Fragile X Syndrome. Neuron 87, 699–715. [PubMed: 26291156]
75. Port RG, Gandal MJ, Roberts TPL, Siegel SJ, and Carlson GC (2014). Convergence of circuit dysfunction in ASD: a common bridge between diverse genetic and environmental risk factors and common clinical electrophysiology. Front. Cell. Neurosci. 8, 414. [PubMed: 25538564]
76. Van Overwalle F, De Coninck S, Heleven E, Perrotta G, Taib NOB, Manto M, and Mariën P. (2019). The role of the cerebellum in reconstructing social action sequences: a pilot study. Soc. Cognit. Affect Neurosci. 14, 549–558. [PubMed: 31037308]
77. Buckner RL, Krienen FM, Castellanos A, Diaz JC, and Yeo BTT (2011). The organization of the human cerebellum estimated by intrinsic functional connectivity. J. Neurophysiol. 106, 2322–2345. [PubMed: 21795627]
78. Stoodley CJ, and Schmahmann JD (2010). Evidence for topographic organization in the cerebellum of motor control versus cognitive and affective processing. Cortex 46, 831–844. [PubMed: 20152963]
79. Badura A, Verpeut JL, Metzger JW, Pereira TD, Pisano TJ, Deverett B, Bakshinskaya DE, and Wang SSH (2018). Normal cognitive and social development require posterior cerebellar activity. Elife 7, e36401.
80. Popa LS, Hewitt AL, and Ebner TJ (2013). Purkinje Cell Simple Spike Discharge Encodes Error Signals Consistent with a Forward Internal Model. Cerebellum 12, 331–333. [PubMed: 23361619]
81. Shadmehr R, and Holcomb HH (1997). Neural correlates of motor memory consolidation. Science 277, 821–825. [PubMed: 9242612]
82. Tseng Y. w., Diedrichsen J, Krakauer JW, Shadmehr R, and Bastian AJ (2007). Sensory Prediction Errors Drive Cerebellum-Dependent Adaptation of Reaching. J. Neurophysiol. 98, 54–62. [PubMed: 17507504]
83. Stoodley CJ, and Tsai PT (2021). Adaptive Prediction for Social Contexts: The Cerebellar Contribution to Typical and Atypical Social Behaviors. Annu. Rev. Neurosci. 44, 475–493. [PubMed: 34236892]
84. Carta I, Chen CH, Schott AL, Dorizan S, and Khodakhah K. (2019). Cerebellar modulation of the reward circuitry and social behavior. Science 363, eaav0581.
85. Hull C. (2020). Prediction signals in the cerebellum: beyond supervised motor learning. Elife 9, e54073.
86. McAfee SS, Liu Y, Sillitoe RV, and Heck DH (2021). Cerebellar Coordination of Neuronal Communication in Cerebral Cortex. Front. Syst. Neurosci. 15, 781527.
87. Popa D, Spolidoro M, Proville RD, Guyon N, Belliveau L, and Léna C. (2013). Functional role of the cerebellum in gamma-band synchronization of the sensory and motor cortices. J. Neurosci. 33, 6552–6556. [PubMed: 23575852]
88. McAfee SS, Liu Y, Sillitoe RV, and Heck DH (2019). Cerebellar Lobulus Simplex and Crus I Differentially Represent Phase and Phase Difference of Prefrontal Cortical and Hippocampal Oscillations. Cell Rep. 27, 2328–2334.e3. [PubMed: 31116979]
89. Mientjes EJ, Nieuwenhuizen I, Kirkpatrick L, Zu T, Hoogeveen-Westerveld M, Severijnen L, Rifé M, Willemsen R, Nelson DL, and Oostra BA (2006). The generation of a conditional Fmr1 knock out mouse model to study Fmrp function in vivo. Neurobiol. Dis. 21, 549–555. [PubMed: 16257225]
90. Barski JJ, Dethleffsen K, and Meyer M. (2000). Cre recombinase expression in cerebellar Purkinje cells. Genesis 28, 93–98. [PubMed: 11105049]
91. Hunter JE, Berry-Kravis E, Hipp H, and Todd PK (1993). FMR1 Disorders. In GeneReviews(®), Adam MP, Ardinger HH, Pagon RA, Wallace SE, Bean LJH, Gripp KW, Mirzaa GM, and Amemiya A, eds.
92. Quiroga RQ, Nadasdy Z, and Ben-Shaul Y. (2004). Unsupervised spike detection and sorting with wavelets and superparamagnetic clustering. Neural Comput. 16, 1661–1687. [PubMed: 15228749]
93. Roth BL (2016). DREADDs for Neuroscientists. Neuron 89, 683–694. [PubMed: 26889809]

94. Buitrago MM, Schulz JB, Dichgans J, and Luft AR (2004). Short and long-term motor skill learning in an accelerated rotarod training paradigm. Neurobiol. Learn. Mem. 81, 211–216. [PubMed: 15082022]

95. Silverman JL, Yang M, Lord C, and Crawley JN (2010). Behavioural phenotyping assays for mouse models of autism. Nat. Rev. Neurosci. 11, 490–502. [PubMed: 20559336]

96. Yang M, Silverman JL, and Crawley JN (2011). Automated three-chambered social approach task for mice. Curr. Protoc. Neurosci. Chapter 8. Unit-8.26.

97. Yang M, and Crawley JN (2009). Simple behavioral assessment of mouse olfaction. Curr Protoc Neurosci Chapter. Curr. Protoc. Neurosci. Chapter 8. Unit 8 24.

98. McFarlane HG, Kusek GK, Yang M, Phoenix JL, Bolivar VJ, and Crawley JN (2008). Autism-like behavioral phenotypes in BTBR T+tf/J mice. Gene Brain Behav. 7, 152–163.

99. Roullet FI, and Crawley JN (2011). Mouse models of autism: testing hypotheses about molecular mechanisms. Curr. Top. Behav. Neurosci. 7, 187–212. [PubMed: 21225409]

100. Ronesi JA, Collins KA, Hays SA, Tsai NP, Guo W, Birnbaum SG, Hu JH, Worley PF, Gibson JR, and Huber KM (2012). Disrupted Homer scaffolds mediate abnormal mGluR5 function in a mouse model of fragile X syndrome. Nat. Neurosci. 15, 431–440. [PubMed: 22267161]

101. Guo W, Molinaro G, Collins KA, Hays SA, Paylor R, Worley PF, Szumlinski KK, and Huber KM (2016). Selective Disruption of Metabotropic Glutamate Receptor 5-Homer Interactions Mimics Phenotypes of Fragile X Syndrome in Mice. J. Neurosci. 36, 2131–2147. [PubMed: 26888925]

Highlights

- Loss of cerebellar *Fmr1* contributes to cerebellar dysfunction and ASD-relevant phenotypes
- Re-expression of cerebellar *Fmr1* benefits observed global KO phenotypes
- Targeting domain Crus1 improves observed phenotypes in cerebellar and global *Fmr1* models

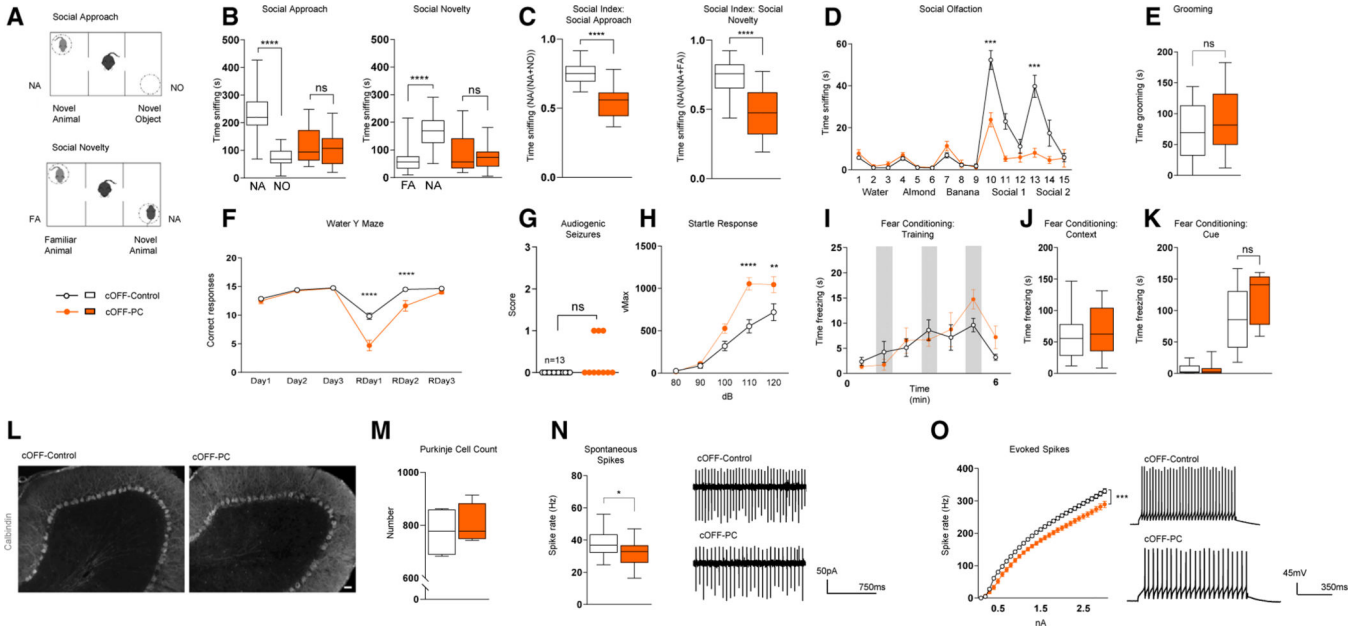

Figure 1. *Fmr1* is necessary for social behaviors and PC function

(A) Diagram of three-chamber social approach and social novelty behavior test.

(B–D) Time spent investigating social stimuli in (B) social approach and social novelty, (C) social index, and (D) social olfactory assays.

(E) Time spent grooming was observed for a period of 10 min.

(F) In the water Y maze, the frequency of correct responses was recorded.

(G) Audiogenic seizures were scored between groups: 0 = no response; 1 = wild running; 2 = tonic-clonic seizures; and 3 = status epilepticus/death.

(H) Startle response was tested between groups.

(I–K) Fear conditioning tests: mice were trained to associate a tone with a shock (gray boxes denote tone/shock pair), and then their learned response was observed in (J) context and (K) cued assays.

(L and M) Cerebellar sections were stained with anti-calbindin (L) and PC number was quantified per whole slice (M). n = 4.

(N and O) Spontaneous firing rate (N) and evoked spike rate (O) were recorded from PCs via whole-cell patch clamp.

Box line denotes median, and whiskers denote 5%–95%. Two-way ANOVA, Bonferroni post hoc analysis. *p < 0.05, **p < 0.01, ***p < 0.001, and ****p < 0.0001. FA, familiar animal; NA, novel animal; NO, novel object; ns, not significant; RDay, reversal day. Data are reported as mean ± SEM. n ≥ 8 for all behavioral studies. Scale bar: 100 μm. Complete p values and animal numbers can be found in Table S1.

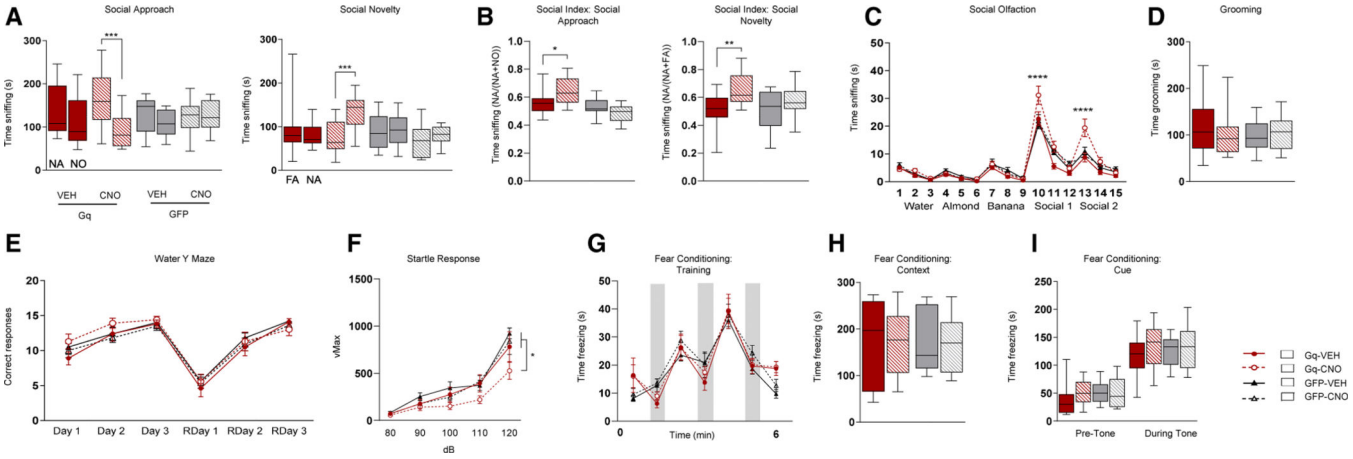

Figure 2. Stimulation of PC activity in RCrus1 is sufficient to improve social preference in PC *Fmr1* mutants

(A–C) Time spent sniffing in the three-chamber following CNO or VEH administration in Gq-DREADD- and GFP-infected groups (A) social approach and social novelty, (B) social index, and (C) social olfaction.

(D and E) Repetitive grooming (D) and reversal learning (E) behaviors in the water Y maze were observed.

(F) Acoustic startle response was tested across all groups.

(G–I) 3-day fear conditioning tasks were evaluated: (G) training (gray boxes denote tone/shock pair), (H) context, or (I) cue. All behavior experiments include Gq DREADD-injected and GFP-injected cOFF-PC mutants and include both CNO and VEH conditions. Learning tasks (water Y maze and fear conditioning) used separate cohorts for VEH and CNO to control for learned behaviors.

Box line denotes median, and whiskers denote 5%–95%. Two-way ANOVA, Bonferroni post hoc analysis. *$p < 0.05$, **$p < 0.01$, ***$p < 0.001$, and ****$p < 0.0001$. CNO, clozapine-N-oxide; VEH, vehicle; FA, familiar animal; NA, novel animal; NO, novel object; RDay, reversal day; ns, not significant. Data are reported as mean ± SEM. $n \geq 10$ for all groups. Complete p values and animal numbers can be found in Table S2.

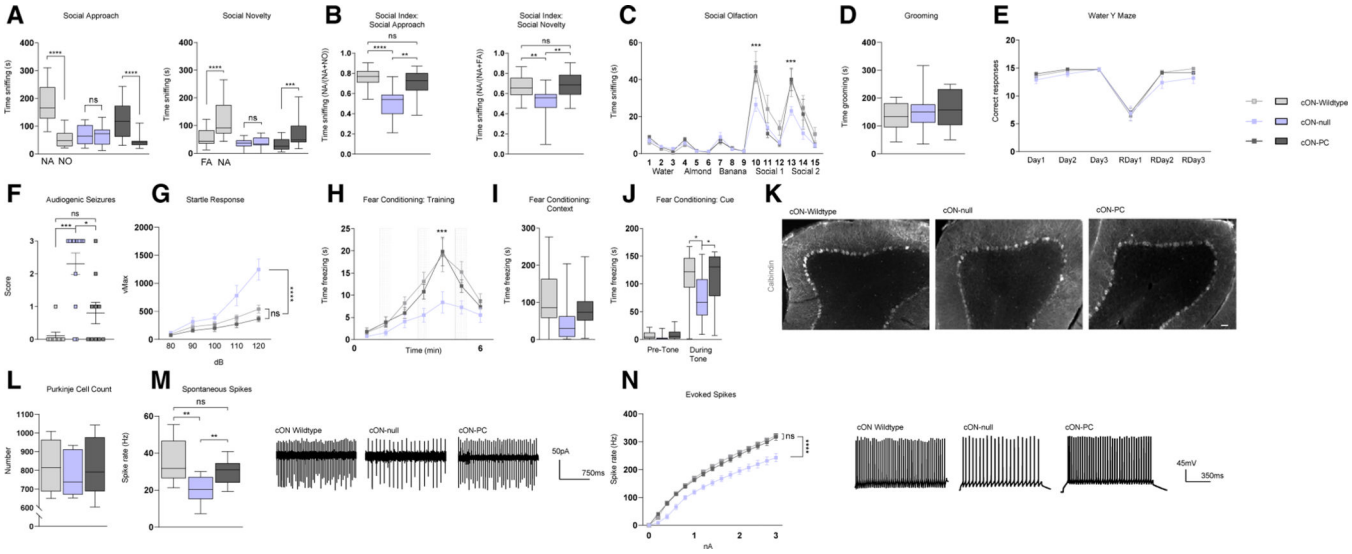

Figure 3. PC expression of *Fmr1* is sufficient to prevent social deficits and PC dysfunction in constitutive *Fmr1* mutants

(A–C) Time spent sniffing in (A) social approach and novelty, (B) social index, and (C) social olfaction assays was tested across cON-wild-type, cON-null, and cON-PC groups.

(D and E) Time spent grooming (D) and number of correct trials in the water Y maze (E) were recorded between groups.

(F) Audiogenic seizure responses were scored: 0 = no response; 1 = wild running; 2 = tonic-clonic seizures; and 3 = status epilepticus/death.

(G) Acoustic startle response assay was performed as another test of auditory sensitivity.

(H–J) 3-day fear conditioning task was used to evaluate differences in learned fear memory between groups in the (H) training test (gray boxes denote tone/shock pair), (I) context test, (J) and cue test.

(K and L) Anti-calbindin stain was used to identify PC numbers in the cerebellum (K) and subsequently quantified per whole slice (L). (M and N) PC spontaneous firing rates (M) and PC excitability (N) were tested for PC function between groups.

Box line denotes median, and whiskers denote 5%–95%. Two-way ANOVA, Bonferroni post hoc analysis. *$p < 0.05$, **$p < 0.01$, ***$p < 0.001$, and ****$p < 0.0001$. FA, familiar animal; NA, novel animal; NO, novel object; ns, not significant; RDay, reversal day. Data are reported as mean ± SEM. $n \geq 9$ for all behavioral cohorts. Scale bar: 100 μm. Complete p values and animal numbers can be found in Table S3.

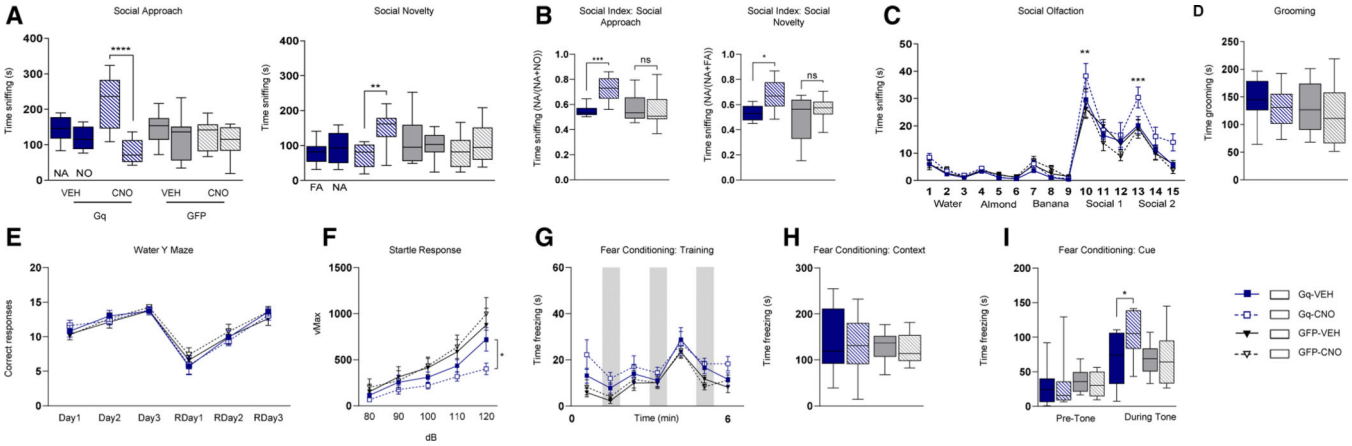

Figure 4. Chemogenetic stimulation of RCrus1 PCs improves behaviors in constitutive *Fmr1* KO mutants

(A–C) Social behaviors were tested and time sniffing was recorded in (A) social approach and novelty, (B) social index, and (C) social olfaction assays across Gq-DREADD- and GFP-infected groups 30 min after CNO or VEH was administered.

(D and E) Time spent grooming (D) and number of correct trials in the water Y maze (E) did not differ between groups.

(F) Following CNO or VEH administration, startle response was compared across infection and treatment groups.

(G–I) A 3-day fear conditioning task: (G) training (gray boxes denote tone/shock pair), (H) context, and (I) cue assays tested for differences in learned fear responses between infection and treatment groups. All behavior experiments include Gq DREADD-injected and GFP-injected cON-null mutants and include both CNO and VEH conditions. Learning tasks (water Y maze and fear conditioning) used separate cohorts for VEH and CNO to control for learned behaviors.

Box line denotes median, and whiskers denote 5%–95%. Two-way ANOVA, Bonferroni post hoc analysis. *$p < 0.05$, **$p < 0.01$, ***$p < 0.001$, and ****$p < 0.0001$. CNO, clozapine-N-oxide; VEH, vehicle; FA, familiar animal; NA, novel animal; NO, novel object; RDay, reversal day; ns, not significant. Data are reported as mean ± SEM. $n \geq 8$ for all groups. Complete p values and animal numbers can be found in Table S4.

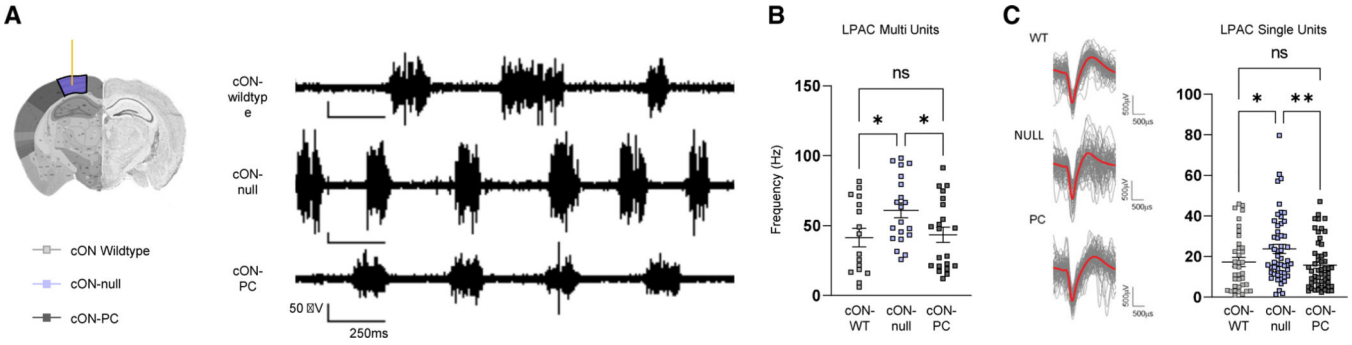

Figure 5. Cerebellar *Fmr1* reduces LPAC hyperexcitability

(A) Schematic of electrode placement in LPAC layer 4 and representative traces from cON-wild-type, cON-null, and cON-PC mice.

(B and C) Multi- (B) and single-unit (C) analysis of anesthetized *in vivo* recording of the LPAC. The waveforms on the left (C) reflect the first 100 assigned to a single unit (gray) with a superimposed average waveform (red).

Two-way ANOVA, Bonferroni post hoc analysis. *$p < 0.05$ and **$p < 0.01$. Data are reported as mean ± SEM. $n \geq 10$ for all groups. Complete p values and animal numbers can be found in Table S5.

KEY RESOURCES TABLE

REAGENT or RESOURCE	SOURCE	IDENTIFIER
Antibodies		
Calbindin	Abcam	Abcam Cat# ab108404, RRID:AB_10861236
Calbindin	Sigma	Sigma-Aldrich Cat# C9848, RRID:AB_476894
FMRP	Developmental Studies Hybridoma Bank	DSHB Cat# 2F5–1, RRID:AB_10805421
Bacterial and virus strains		
AAV8-CamKIIa-hM3D(Gq)-mCherry	Addgene	50476
AAV8-CamKIIa-eGFP	Addgene	50469
Chemicals, peptides, and recombinant proteins		
TTX	Abcam	AB120054
R-CPP	Tocris	0247/10
NBQX	Sigma	N183
Picrotoxin	Tocris	1128
Experimental models: Organisms/strains		
Fmr1 floxed (cOFF) mice	c/o David Nelson	N/A
Fmr1 cON mice	c/o David Nelson	N/A
L7Cre mice	The Jackson Laboratory	004146
Oligonucleotides		
cOFF F-genotyping: GCCTCACATCCTAGCCCTCTAC	Mientjes et al.[89]	N/A
cOFF R-genotyping: CCCACAAAGTTGATTCCCCAGA	Mientjes et al.[89]	N/A
cON F- genotyping: GllGAGCGGCCGAGlllGTCAG	Guo et al.[10]	N/A
cON R- genotyping: GAGATCAGCAGCCTCTGllCCACA	Guo et al.[10]	N/A
Software and algorithms		
ImageJ	NIH	https://imagej.net/RRID:SCR_003070
PRISM	Graphpad 9.3.1.471	https://www.graphpad.com/scientific-software/prism/
MATLAB	MathWorks R2020b	http://www.mathworkm.com/products/matlma/RRID:SCR_001622
Image Lab	Bio-Rad 6.1	http://www.bio-rad.com/enus/sku/1709690-image-lab-softwareRRID:SCR014210
Zen lite	Zeiss 6.2.9200.0	https://www.zeiss.coc/microscopy/us/proprodu/microscope-software/zen-lite.htmlRRID:SCR_018163
pClamp 10	Axon Instruments	http://www.moleculermoleul.com/productp/software/pclamp.hthtRRID:SCR011323

REAGENT or RESOURCE	SOURCE	IDENTIFIER
Zenodo DOI	Github	https://doi.org/10.5281/zenodo.10092944https://doi.org/10.5281/zenodo.10092944